Mol. Cells *34*, 349-355, October 31, 2012
DOI/10.1007/s10059-012-2247-8
pISSN: 1016-8478 eISSN: 0219-1032

Molecules and Cells
http://molcells.org

Functional and Structural Effects of Amyloid-β Aggregate on *Xenopus laevis* Oocytes

Jorge Parodi[1,2], Lenin Ochoa-de la Paz[2], Ricardo Miledi[2], and Ataúlfo Martínez-Torres[2,*]

***Xenopus laevis* oocytes exposed to amyloid-β aggregate generated oscillatory electric activity (*blips*) that was recorded by two-microelectrode voltage-clamp. The cells exhibited a series of "spontaneous" blips ranging in amplitude from 3.8 ± 0.9 nA at the beginning of the recordings to 6.8 ± 1.7 nA after 15 min of exposure to 1 μM aggregate. These blips were similar in amplitude to those induced by the channel-forming antimicrobial agents amphotericin B (7.8 ± 1.2 nA) and gramicidin (6.3 ± 1.1 nA). The amyloid aggregate-induced currents were abolished when extracellular Ca^{2+} was removed from the bathing solution, suggesting a central role for this cation in generating the spontaneous electric activity. The amyloid aggregate also affected the Ca^{2+}-dependent Cl^- currents of oocytes, as shown by increased amplitude of the transient-outward chloride current (T_{out}) and the serum-activated, oscillatory Cl^- currents. Electron microcopy revealed that amyloid aggregate induced the dissociation of the follicular cells that surround the oocyte, thus leading to a failure in the electro-chemical communication between these cells. This was also evidenced by the suppression of the oscillatory Ca^{2+}-dependent ATP-currents, which require proper coupling between oocytes and the follicular cell layer. These observations, made using the *X. laevis* oocytes as a versatile experimental model, may help to understand the effects of amyloid aggregate on cellular communication.**

INTRODUCTION

Alzheimer's disease (AD) is a progressive and irreversible neurodegenerative disorder that leads to major debilitating cognitive deficits in the elderly (Selkoe, 2002). New advances have deciphered several mechanisms that induce AD, but many remain largely unknown, slowing the development of new therapies (Roberson and Mucke, 2006).

AD patients show abnormal accumulation of amyloid-β (Aβ) peptides. When these peptides are overproduced or are not properly cleaved, they spontaneously self-aggregate into assemblies that range from oligomers to protofibrils, fibrils, and amyloid plaques (Haass and Selkoe, 2007). One of the main working hypotheses for the origin of AD is that Aβ aggregate either: i) binds to membrane receptors affecting their functions (Bourin et al., 2003), ii) interferes with signaling cascades (Daniels et al., 2001; Maccioni et al., 2001) or, iii) directly disrupts neuronal membranes by generating pores that lead to major changes in ionic homeostasis (Arispe et al., 1994; Jang et al., 2007). The latter hypothesis is supported by several lines of evidence, including the finding that the Aβ (1-40) peptide undergoes a supramolecular conformational change, forming structures that resemble ion channels which, in turn, have the ability to generate ion-currents in reconstituted, synthetic membranes (Quist et al., 2005). Other studies have suggested that Aβ aggregate alter synaptic function of hippocampal neurons maintained in culture due to changes in either neurotransmitter-receptor trafficking and/or release frequency of synaptic vesicles (Avila et al., 2010; Hsieh et al., 2006; Shankar et al., 2007). All of these modifications are closely associated with deregulation of intracellular Ca^{2+} (Mattson and Chan, 2001). In addition, previous findings (Arispe et al., 1994) suggested the possibility that amyloid aggregate can form or induce the formation of a membrane pore selective for Ca^{2+}. This idea has been tested in hippocampal neurons in culture, and it was demonstrated that amyloid aggregate allow the entry of Ca^{2+} into the cells, leading to neuronal death (Sepulveda et al., 2010).

The *X. laevis* oocyte is surrounded by several layers of follicular and epithelial cells that are electrically and chemically coupled (Arellano et al., 1996; Saldana et al., 2009). We show here that exposure of follicles to amyloid aggregate disrupts these contacts, increasing the conductance of the oocyte plasma membrane and physically detaching it from the follicular cells. In addition, the amyloid aggregate induces changes in the basal electric noise of the oocyte plasma membrane, generating spontaneous electrical events (blips) that depend on extracellular Ca^{2+}. In previous reports, ion channels and neurotransmitter receptors, heterologously expressed in oocytes, were shown to be modulated by Aβ-amyloid (Mezler et al., 2012; Pandya and Yakel, 2011; Texido et al., 2011). Thus, we propose the use of frog oocyte and follicles as experimental models to determine electric changes induced by amyloid ag-

[1]Laboratorio de Fisiología de la Reproducción, Núcleo de Producción Alimentaria, Escuela de Medicina, Veterinaria, Facultad de Recursos Naturales, Universidad Católica de Temuco, Temuco, Chile, [2]Laboratorio de Neurobiología Molecular y Celular, Departamento de Neurobiología Celular y Molecular, Instituto de Neurobiología, Campus Juriquilla-Querétaro, UNAM, México
*Correspondence: ataulfo@unam.mx

Received November 1, 2011; revised August 22, 2012; accepted September 5, 2012; published online October 18, 2012

Keywords: Alzheimer's disease, ATP-currents, transient-outward chloride current, voltage-Clamp

gregate. This approach will potentially speed up the screening for drugs against amyloid aggregation and its action on membranes.

MATERIALS AND METHODS

Amyloid aggregation

Human synthetic $A\beta_{1-40}$ peptides were dissolved in dimethyl sulfoxide (DMSO) at a concentration of 10 mg/ml and immediately stored in aliquots at -20°C. Twenty-five μl of this Aβ-peptide stock solution (10 mg/ml) was diluted to a final concentration of 80 μM in 725 μl of PBS (Tocris Bioscience, USA) and stirred continuously at 200 rpm for 150 min at 37°C (Parodi et al., 2009).

Electrophysiological recordings and transmission electron microscopy

All the animals were handled in accordance with the guidelines of the National Institutes of Health Guide for Care and Use of Laboratory Animals and with the approval of the Institutional Animal Care and Use Committee of the National University of Mexico. *X. laevis* frogs were anesthetized with 0.1% 3-aminobenzoic acid methylester (MS-222) for 10 min, and follicles were isolated manually using fine-tipped forceps. To determine the effect of amyloid aggregate on endogenous oocyte currents, the cells were treated with 0.3 μg/μl collagenase type I at room temperature for 35 min to remove the follicular cell layer, and then kept at 16°C in Barth's medium: 88 mM NaCl, 1 mM KCl, 0.33 mM $Ca_2(NO)_3$, 0.41 mM $CaCl_2$, 0.82 mM $MgSO_4$, 2.4 mM $NaHCO_3$, 5 mM HEPES, pH 7.4, containing 0.1 mg/ml gentamycin sulfate. The electrophysiological recordings were obtained 24 h after isolation.

For electrophysiological recordings, two electrodes were inserted into the oocyte, and membrane currents were recorded in the voltage-clamp configuration at -60 mV (Miledi, 1982). The cells were superfused with frog Ringer's solution: 115 mM NaCl, 2 mM KCl, 1.8 mM $CaCl_2$, 5 mM HEPES, pH 7.4, at room temperature (20-25°C). Gramicidin (100 μg/μl), amphotericin-B (250 μg/μl), or amyloid aggregate (Aβ) (1 μM or 22 μg/μl) were perfused while recording the resting membrane potential for 15 min. To test the role of extracellular cations on the effect of amyloid aggregate, we substituted the Na^+, K^+, or Ca^{2+} in the Ringer's solution. Na^+ was partially replaced by N-Methyl-D-glucamine ($NMDG^+$ 50%), K^+ by an equimolar concentration of CsCl (100%), and Ca^{2+} by Mg^{2+} (5 mM). High Ca^{2+} Ringer's was prepared by increasing the concentration of Ca^{2+} to 10 mM.

To determine the effect of the amyloid aggregate on the electrical coupling between oocytes and surrounding follicular cells, follicles were exposed to 100 μM ATP to induce the oscillatory, Ca^{2+}-dependent Cl^- current (Arellano et al., 1996; 1998) before and after a 15-min exposure to amyloid aggregate. After electrophysiological recordings, the oocytes were processed for electron microscopy (Saldana et al., 2009) by fixation in 4% glutaraldehyde, and embedded in the plastic resin "EPOL"; slices of 2 μm were obtained, contrasted with 2% uranyl acetate, placed on lead grids, rinsed, and observed under the electron microscope (JEOL JEM 1010, JEOL Ltd., Japan).

Data analysis

Spontaneous electrical events of the oocyte plasma membrane were recorded for 15 min in the presence or not of amyloid aggregate (22 μM), amphotericin B (200 μM), or gramicidin (100 μM). The frequency of blips was analyzed using the Root Mean Square (RMS) tool of Mini Analysis 6 Software and plotted using pClampfit 9; the membrane conductance was determined as previously described (Reiser and Miledi, 1989), and the variance of the events and average decay constants (τ) were derived and are shown in Table 1. To determine what ion is responsible for generating the blips, the current-voltage relation of blips was constructed by applying a pulse protocol from -150 mV to 60 mV.

Table 1. Decay constants (τ) and amplitude variance of blips in the absence or presence of amyloid aggregate in normal or in Ca^{2+}-free Ringer's, amphotericin B, and gramicidin

Condition	τ (ms)	Variance (nA)
Control	1,900 ± 1,000	0.7 ± 0.01
Gramicidin	0.004 ± 0.0002	7.2 ± 0.12
Amphotericin B	0.01 ± 0.0004	1.6 ± 0.03
Amyloid aggregate Ca^{2+} free	100 ± 10	1 ± 0.01
Amyloid aggregate	0.03 ± 0.0005	7.3 ± 0.1

Recordings were acquired using a Warner amplifier (OC-765C, Warner Instruments, LLC., USA) and an AC/DC converter (Digidata 1322A, Axon, Molecular Devices, USA) and stored in winWCP. Files were analyzed and plotted using pClampfit 9 (Axon, Molecular Devices, USA) and Origin 8.0. ANOVA (confidence interval of 95%) was used to analyze multiple means and was followed by Bonferroni's test to correct for type I errors. Student's *t*-test with confidence interval of 95% was used to compare the means of controls versus experimental conditions.

RESULTS

Blips of oocytes exposed to membrane-perforating molecules and amyloid aggregate

The stability of the oocyte plasma membrane was assessed by recording the basal electric activity of cells held at -60 mV for periods of 15 min before adding any substances. During these recordings the spontaneous activity was minimal in control cells, and the amplitude of the blips fluctuated from 3.8 ± 0.9 nA at the beginning to 4.5 ± 0.8 nA at the end of the recording. In contrast, the spontaneous activity increased greatly when gramicidin (100 μg/μl) or amphotericin B (250 μg/μl) were superfused onto the oocytes, and at the end of the recording time-lapse we found that the amplitude of blips increased to an average of 7.8 ± 1.2 nA for gramicidin and 6.3 ± 1.1 nA for amphotericin B (Fig. 1A and plotted in 1B). Furthermore, when oocytes were bathed in a 1 μM solution of amyloid aggregate for 15 min, the amplitude of blips increased to an average of 6.8 ± 1.7 nA, *i.e.*, a value very similar to that generated by the other molecules.

The amplitude of blips from the control cells was concentrated near -2.5 nA; in contrast, amyloid aggregate, gramicidin, or amphotericin induced blips with a broad range of ampltitudes, ranging from -6 to +0.5 nA (Fig. 2A). The membrane conductance increased when cells were exposed to each of the three molecules tested, from an average of -141 ± 14 nS in control samples to -647 ± 78, -522 ± 51, and -577 ± 25 nS for gramicidin, amphotericin B, and amyloid aggregate, respectively (Fig. 2B). Current-voltage relations were constructed to gain some understanding of the ion(s) responsible for the currents observed. The plot in Fig. 2C shows an almost linear relation for all the conditions and voltages tested. Gramicidin and amyloid

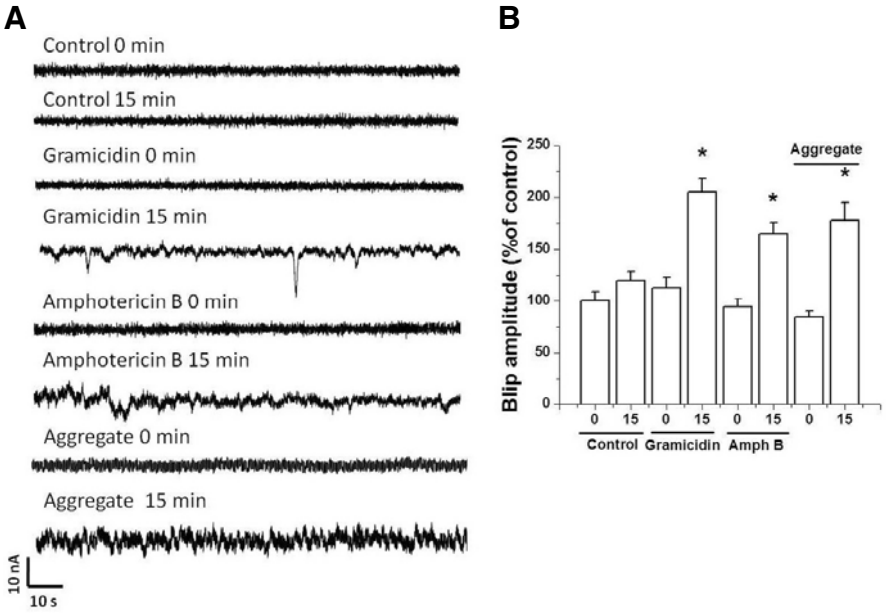

Fig. 1. Spontaneous electric blip activity of *X. laevis* oocytes. (A) Sample recordings from oocytes exposed to gramicidin (100 μg/μl), amphotericin-B (250 μg/μl), or amyloid aggregate (1 μM). (B) Average amplitude of blip currents from sample traces (% of control). Each bar (mean ± SEM) was obtained from at least six different cells. Amph B, amphotericin B. The asterisk indicates $P < 0.05$ (ANOVA).

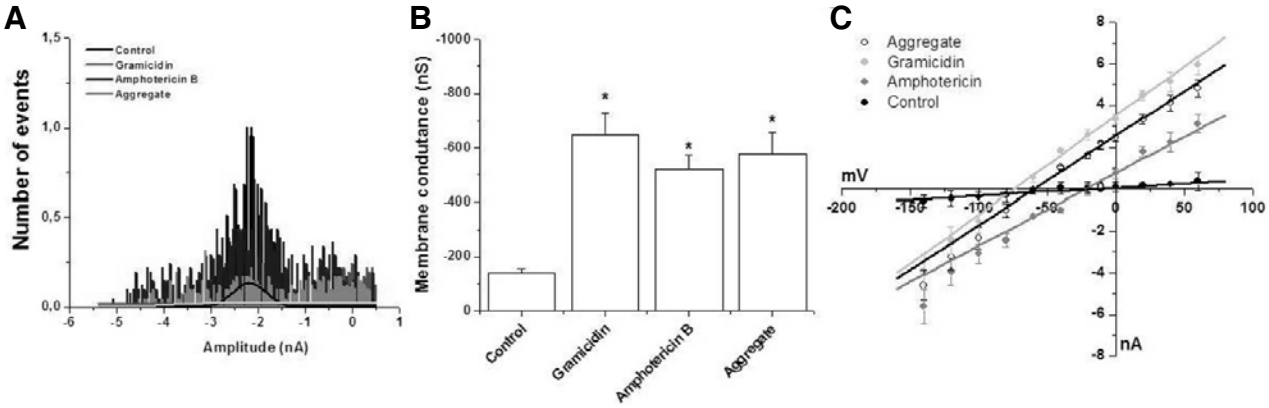

Fig. 2. Distribution of blip amplitudes and current-voltage relation. (A) Histogram distribution of frequencies of blip amplitudes from oocytes exposed to amyloid aggregate, gramicidin, or amphotericin. (B) Bar graph of average membrane conductance in different conditions. Each bar (mean ± SEM) represents measurements of at least six different oocytes. The asterisks indicate $P < 0.05$ (ANOVA). (C) Current-voltage relations for blip amplitude at different voltages in the presence of amyloid aggregate, gramicidin, or amphotericin.

aggregate showed reversal potentials of -51 ± 5 mV and -69 ± 4 mV, respectively (Fig. 2C), suggesting a cationic conductance near the equilibrium potential for Ca^{2+} in oocytes bathed in Ringer's, although other conductances cannot be excluded.

The observations above suggested that the amyloid aggregate could be inducing pores in the plasma membrane of the oocyte; thus, we examined the effect of removing extracellular Ca^{2+} on the generation of spontaneous activity. Ca^{2+}-free Ringer's was superfused onto the oocytes either in the presence or absence of 1 μM amyloid aggregate. When Ca^{2+} was removed from the extracellular medium of the oocytes, the amyloid aggregate did not elicit evident changes in the amplitude of blips as compared to control oocytes bathed in normal Ringer's solution (11.5 ± 1.7 *vs.* 12.3 ± 1.1 nA, respectively; Fig. 3A, Student's *t*-test, $p < 0.05$; control *vs.* normal Ringer's). Perfusion of 1 μM amyloid aggregate for 15 min in normal Ringer's increased the amplitude to 21.8 ± 1.3 nA; in sharp contrast, in Ca^{2+}-free Ringer's the amyloid aggregate did not increase the amplitude of blips, which remained at the same levels as in control cells (12.6 ± 1.7 nA, Fig. 3B, Student's *t*-test, $p < 0.05$; control *vs.* Ca^{2+} free Ringer's). This observation suggests that extracellular Ca^{2+} generates, at least in part, the blips induced by amyloid aggregate.

We explored the effect of reducing Na^+ or K^+ in the Ringer's solution on blip amplitude in the presence of amyloid aggregate. In both cases we observed slight increases in the amplitudes of the blips, also these increases were statistically significant when compared to the effect of the amyloid aggregate in normal Ringer's (indicated as ρ's in Fig. 3C), however all groups showed differences when compared to the untreated control (indicated as * in Fig. 3C ANOVA, $p < 0.05$). Oocytes exhibit endogenous conductances generated by entry of extracellular Ca^{2+} as well as by Ca^{2+} released from intracellular stores; for example the depolarization-induced T_{out} current (Miledi, 1982)

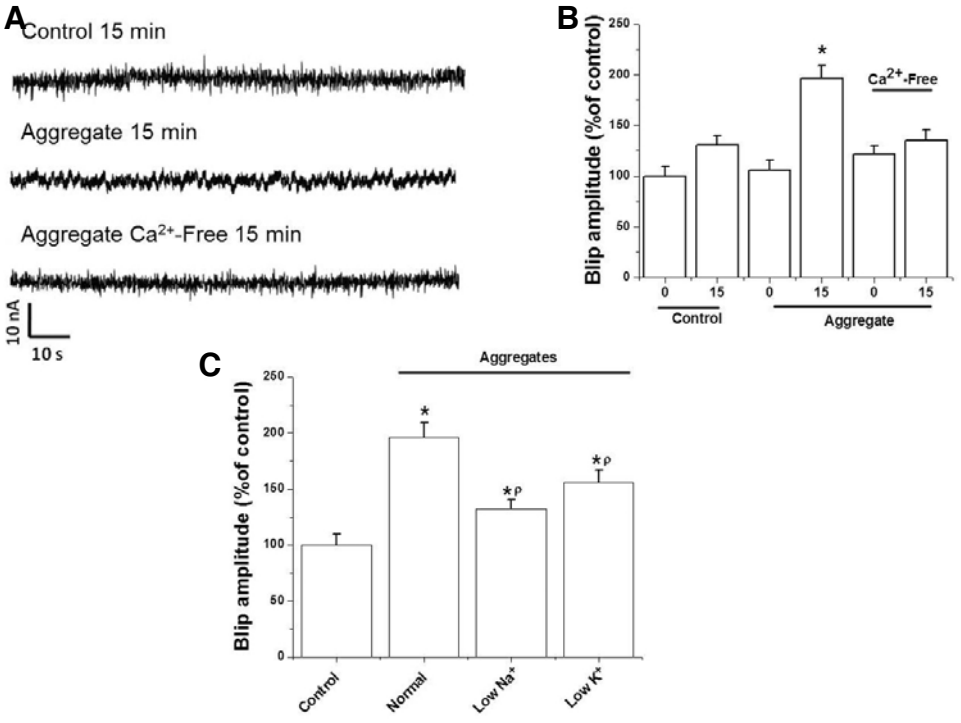

Fig. 3. Ca^{2+}dependence. (A) Sample recordings from an oocyte exposed to amyloid aggregate in the presence or absence of extracellular Ca^{2+} at different times, from 0 to 15 min. (B) Bar graph of average blip amplitudes in Ca^{2+}-free medium. (C) Bar graph for average blip amplitudes and effect of amyloid aggregate with or without Na^{+} or K^{+} solution. Each bar (mean ± SEM) represents measurements of at least six different oocytes. The asterisks (*) indicate significant difference compared to control and ρ's indicate significant difference compared to normal Ringer's solution ($P < 0.05$, ANOVA).

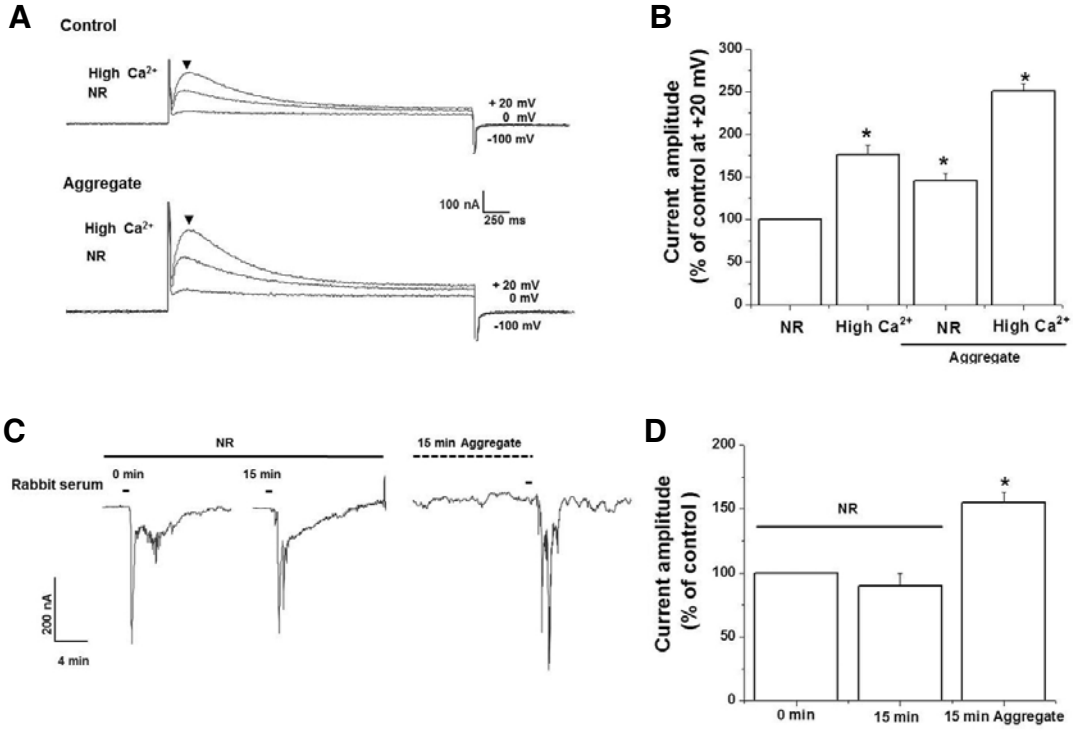

Fig. 4. Effect of amyloid aggregate and extracellular Ca^{2+} on endogenous oocyte currents. (A, B) T_{out} currents in the absence or presence of amyloid aggregate. The high Ca^{2+} media (10 mM) (arrowhead) was used to demonstrate the response of the T_{out} current generated at +20 mV. (B) Bar graph of the current at +20 mV in control and in presence of amyloid aggregate. Observe that amyloid aggregate induces current amplitudes larger than control oocytes. (C) Responses to rabbit serum, in the absence or presence amyloid aggregate. (D) Bar graph for the maximum serum-induced current. Note that the second application (15 min) of serum elicited a smaller response due to receptor desensitization, whereas in cells exposed to amyloid aggregate the response is enhanced. In all these experiments we used oocytes without follicular cells (see "Materials and Methods"). Each bar (mean ± SEM) represents measurements of at least six different oocytes. The asterisks indicate $P < 0.05$ (ANOVA).

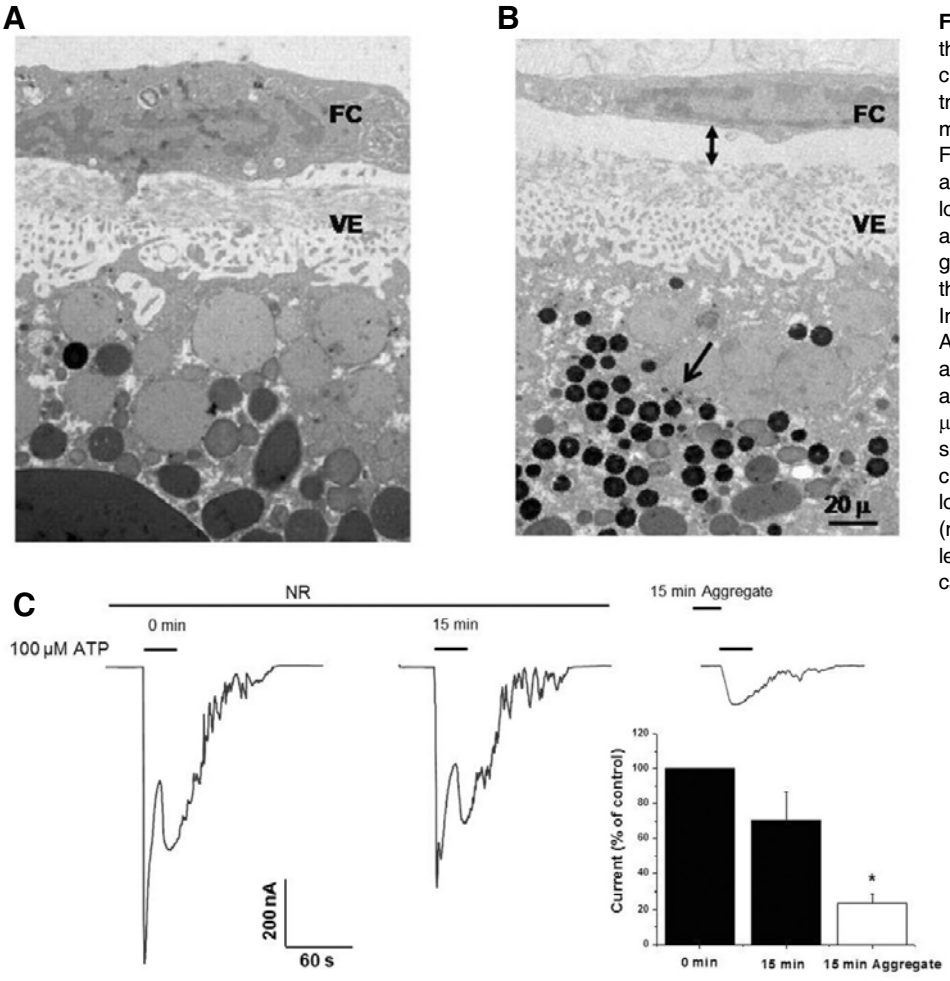

Fig. 5. Amyloid aggregate uncouples the follicular cells. (A) Electron microscopy of a control follicle (A) contrasted with a follicle exposed for 15 min to 1 μM amyloid aggregate (B). Follicular cells (FC) are collapsed and detached from the vitelline envelope (double-headed arrow). The arrow in (B) points to the multiple granules generated after exposing the follicle to the amyloid aggregate. In (C), sample traces of 100 μM ATP-induced currents of follicles at 0 and 15 min under control conditions and after a 15-min incubation with 1 μM amyloid aggregate. The inset plot shows the drop in the ATP-induced currents of follicles exposed to amyloid aggregate. Each bar or dot (mean ± SEM) was measured in a least 6 oocytes. The asterisk indicates $P < 0.05$ (ANOVA).

is a Ca^{2+}-dependent Cl^- current mediated by TMEM16A (Schroeder et al., 2008; Scudieri et al., 2012); this same channel is also responsible for the oscillatory currents generated by serum activation of lysophosphatidic acid (LPA) receptors (Tigyi et al., 1991). We tested the effect of exposing the oocytes to amyloid aggregate for 15 min and observed larger T_{out} currents. This effect was even more evident when high Ca^{2+} Ringer's medium was used in the recording bath (Figs. 4A and 4B), in which the T_{out} current reached up to 200 ± 0.12 nA when oocytes were exposed to the amyloid, *i.e.*, 150% higher than control T_{out} currents. Thus, the high-Ca^{2+} Ringer's consistently increased the T_{out} current by 75 ± 2% compared to the currents reached by oocytes in normal Ringer's, whereas the increases due to the presence of amyloid aggregate were 48 ± 1.9% and 149 ± 3.1%, in normal and high-Ca^{2+} Ringer's, respectively.

To test the effect of amyloid aggregate on the oscillatory Cl^- current elicited by serum activation, we applied rabbit serum (1:100) onto oocytes held at -60 mV, which induced oscillatory currents (Fig. 4C) due to the release of Ca^{2+} from intracellular stores. Two consecutive applications of serum, separated by 15 min, illustrate that there is some receptor desensitization, to 85 ± 3.1% the control; in contrast, when amyloid aggregate are included in the bath, the response to serum increases to about 50 ± 1.8% relative to the control (Figs. 4C and 4D).

Morphological changes and uncoupling of follicular cells

The amyloid aggregate induced several morphological changes in the follicles after 15 min of exposure (Fig. 5). First, the collagen fibers and vitelline envelope were found to be disorganized as compared with the control; second, follicular cells were compacted and frequently detached from the oocyte proper; third, cortical granules were smaller and more numerous in the treated oocytes. Physical detachment of the follicular cells was clearly evident in the EM images, suggesting that the follicular cells had become uncoupled from the oocyte. To explore this idea, we measured the currents induced by ATP in follicles before and after exposure to amyloid aggregate. If the follicular cells were detached, smaller ATP-induced currents would be expected due to a reduction in the number of gap junctions that allow the passage of second messengers from the follicular cells to the oocyte (Miledi and Woodward, 1989). Figure 5C shows sample currents elicited by ATP (100 μM) in control follicles and after 15 min exposure to 1 μM amyloid aggregate. In control oocytes, consecutive applications of 100 μM ATP reduced the currents to 60 ± 12% of the initial response (Fig. 5C, inset), a typical response due to desensitization of the ATP receptors. In contrast, when the follicle was exposed to the amyloid aggregate, the second response to ATP was reduced to 20 ± 4.3% of the first application. This reduction of the ATP-induced current indicates that amyloid aggregate induces the

physical detachment of the follicular cells from the oocyte and thereby disrupts their electrical coupling, as indicated by the reduction of the ATP currents and is consistent with the ultrastructural images.

DISCUSSION

The observations described in this report derive from our finding that *X. laevis* follicles exposed to amyloid aggregate increased their electrical activity, observed as changes in the amplitude of spontaneous activity (blips). One of the fundamental problems to solve in the field of Alzheimer's disease is to elucidate the modes of action of the Aβ peptide; here, we demonstrate the ability of the amyloid aggregate to disrupt the contacts between oocyte and follicular cells, thus uncoupling their electro-chemical communication. This paves the way to use the *Xenopus* follicle as a tool to screen for molecules that could block the action of amyloid aggregate on the plasma membrane.

Amyloid aggregate induces "channel activity" in neurons grown *in vitro* as well as in immortalized cell lines (Kawahara et al., 2000), and more recently, this activity was probed in hippocampal neurons (Sepulveda et al., 2010). In neurons in culture, β-amyloid acts like a pore-forming neurotoxin, increasing intracellular Ca^{2+} and leading to depletion of synaptic vesicles. This observation led us to compare the membrane electric behavior of oocytes exposed to known membrane-perforating agents with that induced by amyloid aggregate. The blips recorded in oocytes exposed to gramicidin, amphotericin B, or amyloid aggregate had similar amplitudes: 7.8, 6.3, and 6.8 nA, respectively, and were clearly larger than those recorded in control cells (4.5 nA). Several studies suggest that amyloid aggregate permit Ca^{2+} entry into the cells and increase membrane conductance in artificial lipid bilayers, clonal cell lines, and neurons in culture (Arispe, 2004; Sepulveda et al., 2010). Furthermore, modifications in the Ca^{2+} concentration are important for developing AD. In the oocyte, the amyloid aggregate induces blips whose reverse equilibrium potential is near to that of Ca^{2+} and whose amplitude is significantly affected by removal of Na^+ or K^+, suggesting that Ca^{2+} is the main ion responsible for these spontaneous electric events, nevertheless other cationic conductances could not be excluded. These observations are consistent with the results showing that reducing extracellular Ca^{2+} decreased the blips generated by amyloid aggregate and have an impact on the oocyte's endogenous, Ca^{2+}-dependent currents, such as the T_{out} and Ca^{2+}- dependent oscillatory Cl^- currents generated by serum. In addition, membrane blips are practically absent when Ca^{2+}- free Ringer´s was used to bathe the oocytes.

Although our results do not show direct evidence for the generation of an Aβ amyloid ion channel, they clearly show the induction of new spontaneous conductances in the plasma membrane of the oocyte and the eventual detachment of follicular cells from the oocyte. Follicular cells were collapsed and separated from the oocyte after only 15 min of contact with amyloid aggregate. Other major structural changes included degeneration of the basal lamina and collapse of intracellular granules within the oocyte. Thus, amyloid aggregate impacted directly the ultrastructure of *X. laevis* follicles, leading to changes in the chemical communication among these cells. This may help to understand how the amyloid aggregate modify, in the short term, the neuronal structure and neurotransmission properties in patients affected by Alzheimer's disease.

Xenopus frog oocytes could be a suitable experimental model for screening drugs that block the effect of amyloid aggregate on the plasma membrane, and may therefore be useful against Alzheimer's disease. This model will enable the study of basic molecular mechanisms associated with amyloid pore formation and its effect on cell to cell communication.

ACKNOWLEDGMENTS

This work was partially supported by grants from CONACYT 101851 and UNAM-PAPIIT 204806 (to AM-T and RM). J.P. is a postdoctoral fellow from CTIC-UNAM and was supported by a travel grant from MECESUP - PUC/0708 of Pontificia Universidad Católica de Chile. The authors thank Dr. D. Pless (INB-UNAM) for editing the manuscript. We are also in debt to E. Ruiz Alcíbar, E. Espino, L. Palma, and E. Pérez for technical assistance. AM-T thanks support from PASPA (Programa de Apoyo para la Superación del Personal Académico-UNAM) for sabatical fellowship. WinWCP was kindly provided by Dr. J. Dempster, University of Strathclyde in Glasgow, U.K.

REFERENCES

Arellano, R.O., Woodward, R.M., and Miledi, R. (1996). Ion channels and membrane receptors in follicle-enclosed *Xenopus* oocytes. Ion Channels *4*, 203-259.

Arellano, R.O., Garay, E., and Miledi, R. (1998). Cl^- currents activated *via* purinergic receptors in *Xenopus* follicles. Am. J. Physiol. *274*, C333-340.

Arispe, N. (2004). Architecture of the Alzheimer's A beta P ion channel pore. J. Membr. Biol. *197*, 33-48.

Arispe, N., Pollard, H.B., and Rojas, E. (1994). The ability of amyloid beta-protein [A beta P (1-40)] to form Ca^{2+} channels provides a mechanism for neuronal death in Alzheimer's disease. Ann. N Y Acad. Sci. *747*, 256-266.

Avila, M.E., Sepulveda, F.J., Burgos, C.F., Moraga-Cid, G., Parodi, J., Moon, R.T., Aguayo, L.G., Opazo, C., and De Ferrari, G.V. (2010). Canonical Wnt3a modulates intracellular calcium and enhances excitatory neurotransmission in hippocampal neurons. J. Biol. Chem. *285*, 18939-18947.

Bourin, M., Ripoll, N., and Dailly, E. (2003). Nicotinic receptors and Alzheimer's disease. Curr. Med. Res. Opin. *19*, 169-177.

Daniels, W.M., Hendricks, J., Salie, R., and Taljaard, J.J. (2001). The role of the MAP-kinase superfamily in beta-amyloid toxicity. Metab. Brain Dis. *16*, 175-185.

Haass, C., and Selkoe, D.J. (2007). Soluble protein oligomers in neurodegeneration: lessons from the Alzheimer's amyloid β-peptide. Nat. Rev. Mol. Cell Biol. *8*, 101-112.

Hsieh, H., Boehm, J., Sato, C., Iwatsubo, T., Tomita, T., Sisodia, S., and Malinow, R. (2006). AMPAR removal underlies Abeta-induced synaptic depression and dendritic spine loss. Neuron *52*, 831-843.

Jang, H., Zheng, J., and Nussinov, R. (2007). Models of beta-amyloid ion channels in the membrane suggest that channel formation in the bilayer is a dynamic process. Biophys. J. *93*, 1938-1949.

Kawahara, M., Kuroda, Y., Arispe, N., and Rojas, E. (2000). Alzheimer's beta-amyloid, human islet amylin, and prion protein fragment evoke intracellular free calcium elevations by a common mechanism in a hypothalamic GnRH neuronal cell line. J. Biol. Chem. *275*, 14077-14083.

Maccioni, R.B., Otth, C., Concha, II., and Munoz, J.P. (2001). The protein kinase Cdk5. Structural aspects, roles in neurogenesis and involvement in Alzheimer's pathology. Eur. J. Biochem. *268*, 1518-1527.

Mattson, M.P., and Chan, S.L. (2001). Dysregulation of cellular calcium homeostasis in Alzheimer's disease: bad genes and bad habits. J. Mol. Neurosci. *17*, 205-224.

Mezler, M., Barghorn, S., Schoemaker, H., Gross, G., and Nim-mrich, V. (2012). Abeta oligomer directly modulates P/Q-type calcium currents in *Xenopus oocytes*. Br. J. Pharmacol. *165*, 1572-1583

Miledi, R. (1982). A calcium-dependent transient outward current in *Xenopus laevis oocytes*. Proc. R Soc. Lond. B. Biol. Sci. *215*, 491-497.

Miledi, R., and Woodward, R.M. (1989). Effects of defolliculation on membrane current responses of *Xenopus oocytes*. J. Physiol.

416, 601-621.
Pandya, A., and Yakel, J.L. (2011). Allosteric modulator Desformylflustrabromine relieves the inhibition of alpha2beta2 and alpha4beta2 nicotinic acetylcholine receptors by beta-amyloid(1-42) peptide. J. Mol. Neurosci. *45*, 42-47.
Parodi, J., Sepulveda, F.J., Roa, J., Opazo, C., Inestrosa, N.C., and Aguayo, L.G. (2009). Beta-amyloid causes depletion of synaptic vesicles leading to neurotransmission failure. J. Biol. Chem. *285*, 2506-2514.
Quist, A., Doudevski, I., Lin, H., Azimova, R., Ng, D., Frangione, B., Kagan, B., Ghiso, J., and Lal, R. (2005). Amyloid ion channels: a common structural link for protein-misfolding disease. Proc. Natl. Acad. Sci. USA *102*, 10427-10432.
Reiser, G., and Miledi, R. (1989). Changes in the properties of synaptic channels opened by acetylcholine in denervated frog muscle. Brain Res. *479*, 83-97.
Roberson, E.D., and Mucke, L. (2006). 100 years and counting: prospects for defeating Alzheimer's disease. Science *314*, 781-784.
Saldana, C., Garay, E., Rangel, G.E., Reyes, L.M., and Arellano, R.O. (2009). Native ion current coupled to purinergic activation *via* basal and mechanically induced ATP release in *Xenopus follicles*. J. Cell. Physiol. *218*, 355-365.
Schroeder, B.C., Cheng, T., Jan, Y.N., and Jan, L.Y. (2008). Expression cloning of TMEM16A as a calcium-activated chloride channel subunit. Cell *134*, 1019-1029.
Scudieri, P., Sondo, E., Ferrera, L., and Galietta, L.J. (2012). The anoctamin family: TMEM16A and TMEM16B as calcium-activated chloride channels. Exp. Physiol. *97*, 177-183.
Selkoe, D.J. (2002). Alzheimer's disease is a synaptic failure. Science *298*, 789-791.
Sepulveda, F.J., Parodi, J., Peoples, R.W., Opazo, C., and Aguayo, L.G. (2010). Synaptotoxicity of Alzheimer beta amyloid can be explained by its membrane perforating property. PLoS One *5*, e11820.
Shankar, G.M., Bloodgood, B.L., Townsend, M., Walsh, D.M., Selkoe, D.J., and Sabatini, B.L. (2007). Natural oligomers of the Alzheimer amyloid-beta protein induce reversible synapse loss by modulating an NMDA-type glutamate receptor-dependent signaling pathway. J. Neurosci. *27*, 2866-2875.
Texido, L., Martin-Satue, M., Alberdi, E., Solsona, C., and Matute, C. (2011). Amyloid beta peptide oligomers directly activate NMDA receptors. Cell Calcium *49*, 184-190.
Tigyi, G., Henschen, A., and Miledi, R. (1991). A factor that activates oscillatory chloride currents in *Xenopus oocytes* copurifies with a subfraction of serum albumin. J. Biol. Chem. *266*, 20602-20609.